# Handling fault in ambient temperature measurements in a cooling system - A fault tolerant control approach

Andreasen, Glenn; Izadi-Zamanabadi, Roozbeh; Stoustrup, Jakob

*Published in:*
IFAC-PapersOnLine

*DOI (link to publication from Publisher):*
10.1016/j.ifacol.2022.07.106



*Publication date:*
2022

*Document Version*
Publisher's PDF, also known as Version of record



*Citation for published version (APA):*
Andreasen, G., Izadi-Zamanabadi, R., & Stoustrup, J. (2022). Handling fault in ambient temperature measurements in a cooling system - A fault tolerant control approach. *IFAC-PapersOnLine*, *55*(6), 61-66. https://doi.org/10.1016/j.ifacol.2022.07.106

Available online at www.sciencedirect.com

ScienceDirect

IFAC PapersOnLine 55-6 (2022) 61–66

# Handling fault in ambient temperature measurements in a cooling system - A fault tolerant control approach ⋆

Glenn Andreasen *,** Roozbeh Izadi-Zamanabadi *,** Jakob Stoustrup *

* Department of Electronic Systems, Aalborg University, 9220 Aalborg, Denmark., (e-mail: ga, riz,Jakob@es.aau.dk)
** Innovation lab, Danfoss A/S, 6430 Nordborg, Denmark. (email: roozbeh@danfoss.com)

**Abstract:** This paper proposes an active fault tolerant control (AFTC) scheme for detecting and correcting faulty measurements from the ambient temperature sensor that is utilized to calculate the optimal setpoints for a rooftop gas cooler unit operation. The faulty measurements are caused by improper placement of the ambient temperature sensor so that it is exposed to heat generated directly or indirectly by the sun. The AFTC is designed in a plug & play manner with no prior knowledge of the underlying system. The underlying system is identified by applying an online identification algorithm. To ensure the validity of the model several criteria is established. The resulting model is utilized in an observer based fault tolerant controller scheme including a bumpless implementation of the fault correction when a fault has been detected. The validity of the proposed AFTC scheme is investigated using both experimental data as well as simulation.



*Keywords:* plug & play, online system identification, refrigeration system, fault tolerant control, ambient temperature

## 1. INTRODUCTION

Fault tolerant control of industrial refrigeration systems is often a challenging task since these systems comprise different configurations, with a varying number of subsystems/components. Furthermore, these factors are often not known prior to the design of the fault tolerant controller schemes. Thus, data-driven methods are an attractive approach to accommodate for the unknown system. Supermarket systems that utilize R744 ($CO_2$) as a refrigerant (henceforth referred to as $CO_2$ supermarket system) are subject to various faults. One of these faults is the effect of insulation on the ambient temperature measurement, which is often not observed but upon occurrence has significant impact on the total system performance. The fault occurs for roof top gas coolers where the ambient temperature sensor is located underneath the gas cooler. Dependent on the location of the gas cooler as well as the sensor's location the sun heats up the roof top and/or the temperature sensor itself. The main reasons for the occurrence of this fault are improper installation (despite the instruction regarding the installation) or the heating of the roof top is simply too high (e.g. consider a dark roof top beneath the gas cooler located in countries with very warm summers). This fault is not directly reported in fault/alarm reports from stores as e.g. documented in Behfar et al. (2018, 2017). As the erroneous temperature sensor measurement is still within the allowed temperature range, no fault is detected and hence no alarm or fault report will be generated. Since the measured ambient temperature is utilized for selecting the reference set-points for the gas-cooler pressure and temperature, the faulty measurement signal causes change in the operating conditions of the total system. Consequently, the plant's coefficient of performance (COP) will be degraded. Unfortunately, no published work was found, which addresses this fault. However, it is well known that the ambient temperature is a limiting factor for the COP. In (Yang et al., 2015; Ge and Tassou, 2011; Kim et al., 2009; Kauf, 1999) several optimal curves for the gas cooler pressure are reviewed where all of them are either directly or indirectly dependent on the ambient temperature. In (Yang et al., 2015) the sensitivity of the COP with respect to changes in temperature and pressure at the outlet of the gas-cooler is clearly demonstrated. This paper proposes an online data-driven active fault tolerant control (AFTC) scheme, which is developed to capture and accommodate faulty measurements from the ambient temperature sensor in refrigeration systems with rooftop condensing units.

The AFTC scheme utilizes an online identification method for estimating the parameters of a linear model for the underlying unknown system, which then provides an estimate of the ambient temperature. The parameters of the model is updated regularly in the periods where healthy measurement readings are available to ensure that the model represents the actual state of the system. The estimated temperature is utilized to detect and compensate the measurement bias in a bump-less manner.

⋆ This work is supported by the Innovation Fund Denmark, 7038-00100B, Denmark.


10.1016/j.ifacol.2022.07.106

In Section 2, the considered system is described from an overview perspective. Section 3 provides the background on the dynamics surrounding the gas cooler and the relevant variables that can be utilized for describing the ambient temperature. Section 4 covers the active fault tolerant controller scheme for accommodating faulty measurements from the ambient temperature sensor. The results are presented in section 5. Finally, the conclusion of the work is provided in section 6.

## 2. THE REFRIGERATION SYSTEM

The considered system is a $CO_2$ supermarket refrigeration system located in Portugal. The simplified version of the system is depicted in Fig. 1, where the most relevant components and measurements for this work are shown. The depicted measurements $T$, $P$, $N$, and $OD$ denotes temperature, pressure, rounds per minute and opening degree respectively. The gas cooler unit in this setup is a V-shaped roof-top air cooled gas cooler, where the ambient temperature sensor is mounted beneath the gas cooler (not in the gas coolers air inlet line).

The cooling process of the refrigerant is realized through control of pressure ($P_{gc}$) and temperature ($T_{gc}$) of the refrigerant at the outlet of the gas cooler. The energy optimal values of these is highly related to the actual ambient temperature. For supermarket refrigeration systems a dedicated "Reference Control" unit calculates the optimal set points for the temperature and pressure of the refrigerant at the outlet of the gas cooler based on the actual ambient temperature readings (see fig. 1).

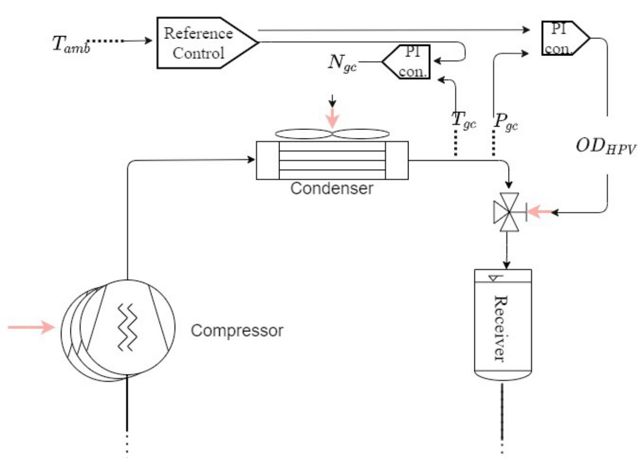


Fig. 1. Illustration of a simplified version of the R744 supermarket refrigeration system and the gas cooler control along with the associated measurements.

It is hence obvious that any faulty or biased measurement of the ambient temperature will have a direct negative impact on the system's energy consumption. The fault is illustrated in Fig. 2, where the top plot shows the measured ambient temperature ($T_{amb,meas}$) and the temperature of the refrigeration at the outlet of the gas cooler ($T_{gc}$). The lower plot shows the fan speed. Besides the regular proportional integrator (PI) controller for controlling the refrigerant temperature at the outlet of the gas cooler there is a logical rule, which sets fan speed to maximum speed when the temperature at the outlet of the gas cooler

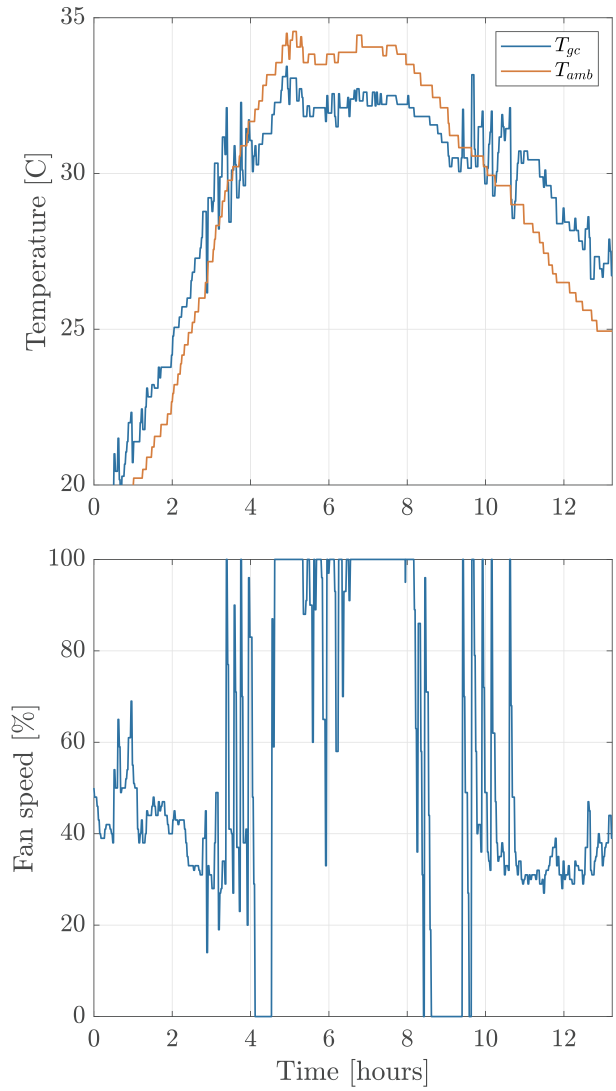


Fig. 2. Illustration of faulty measurements from the ambient temperature sensor, where the top figure shows faulty measurements from ambient temperature sensor ($T_{amb,meas}$) compared with the temperature of the refrigerant at the outlet of the gas cooler ($T_{gc}$). The bottom figure shows the corresponding fan speed.

exceeds 31 $^{o}C$. This explains the jumps in both fan speed and the refrigerant temperature at the outlet of the gas cooler. When the fan speed is running with maximum speed the refrigerant temperature at the outlet of the gas cooler should be roughly equal to or higher than the ambient temperature. However, it can be seen that the refrigerant temperature at the outlet of the gas cooler is lower than the ambient temperature. Physically, in steady state the refrigerant temperature at the outlet of the gas cooler can never be lower than the ambient temperature (when there are no additionally cooling applied to the gas cooler, e.g. water sprayed on the gas cooler). Note that the inlet temperature to the gas cooler is approximately 100 $^{o}C$ during the day and minimum 60 $^{o}C$ during the night in this particular case. When the fan is running at full speed a faulty measurement of the ambient temperature is clearly measured, in this particular day it is approximately

2 °$C$ higher than the temperature of the refrigerant at the outlet of the gas cooler ($T_{gc}$).

The faulty high ambient temperature measurement leads to calculating a higher reference for both pressure and temperature in the "Reference Control" unit. Thus, the effect of the faulty ambient temperature measurement causes a drop in the system's Coefficient-Of-Performance (COP) and a reduction in the fan speed. The reduction of the fan speed may lead to on/off control of the fan, which in turn causes (unnecessary) ripples in pressure and temperature throughout the system. Thereby adding unnecessary degradation of the refrigeration systems components and in severe cases control problems.

## 3. INVESTIGATION OF THE GAS COOLER MODEL

The gas cooler dynamics are investigated to gain insight on what measurements to utilize as input for the system identification method. Fig. 3 illustrates the gas cooler separated in four control volumes for sub-critical refrigerant. The air control volume is the air surrounding the gas cooler, which exchanges heat with the refrigerant inside the gas cooler. The three refrigerant control volumes cover the three refrigerant phases; gas, mixed, and liquid.

In Fig. 3 and throughout this chapter the following assumptions are considered to hold:
- Temperature is the same throughout the individual control volume.
- Thermal conductivity of metal is significantly faster than the thermal conductivity of the refrigerant.
- The dynamics of the ambient temperature sensor is assumed to be negligibly fast and air pressure of the surrounding is constant.

### *3.1 The energy balance equation - air side*

The air side of the gas cooler consists of the air surrounding the metal of the gas cooler.

Furthermore, the air circulation is open to atmospheric pressure. Thus, allowing the energy balance to be described with temperature and specific heat capacity instead of enthalpy:

$$M_{air}C_{air}\frac{d\,T_{air}}{dt} = \dot{m}_{air}C_{air}(T_{amb} - T_{air,o}) + \alpha_l A_l(T_l - T_{air}) + \alpha_g A_g(T_g - T_{air}) + \alpha_{mix}A_{mix}(T_{mix} - T_{air}) \quad (1)$$

where $T_{amb}$ is the air temperature being sucked into the air control volume by the fan, $T_{air}$ is the temperature in the air control volume and $T_{air,o}$ is the air temperature exiting the air control volume. $C_{air}$ is the specific heat capacity of air at atmospheric pressure.

The last 3 terms in Eq. (1) include the variables $T_g$, $T_{mix}$, and $T_{air,o}$, which are not measured in real applications. The problem is remedied by using the following approximation:

$$\alpha_{tot}A_{tot}(T_{gc} - T_{amb}) \approx \alpha_l A_l(T_l - T_{air}) + \alpha_g A_g(T_g - T_{air}) + \alpha_{mix}A_{mix}(T_{mix} - T_{air})$$

where $A_{tot} = A_l + A_{mix} + A_g$ are constant. $\alpha_{tot}$ is the overall heat transfer coefficient and is dependent on the

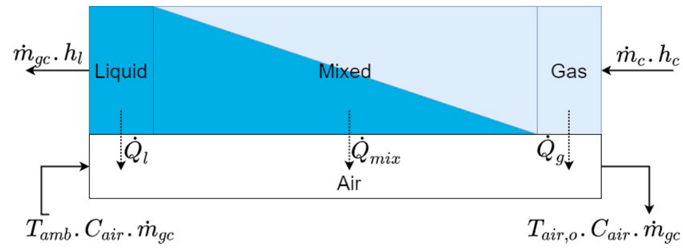


Fig. 3. Illustration of the control volumes for the gas cooler with the refrigerant in subcritical conditions and air surrounding the gas cooler, where the energy flows surrounding the gas cooler are shown.

phase of the refrigerant as well as the mass flow rate of the air and the refrigerant. Furthermore, the temperature in the air control volume ($T_{air}$) is approximated by utilizing the central difference:

$$T_{air} \approx \frac{T_{air,o} + T_{amb}}{2}$$

The outlet air temperature ($T_{air,o}$) is approximated as:

$$T_{air,o} \approx T_{gc} + K_{air,o}$$

where $K_{air,o}$ is a constant in an operating point. Introducing the above mentioned approximations in Eq. (1) results in the following mathematical expression for ambient air dynamics:

$$\frac{d\,T_{amb}}{dt} = \frac{2\cdot\dot{m}_{air}}{M_{air}}(T_{amb} - T_{gc}) + \frac{2\cdot\alpha_{tot}A_{tot}}{M_{air}C_{air}}(T_{gc} - T_{amb}) - \frac{d\,T_{gc}}{dt} - \frac{2\cdot\dot{m}_{air}}{M_{air}}K_{air,o} \quad (2)$$

It is clear that the above equation is non-linear in air mass flow as well as in the overall heat transfer coefficient. The non-linear contribution in Eq. (2) caused by the air mass flow is reduced through the optimal control scheme, which aims at keeping $T_{amb} - T_{gc}$ constant.

The aim is to online construct a (linear) data-driven observer/predictor for the ambient temperature by utilizing a system identification method to capture the dynamic behavior described in Eq. (2).

*Remark*: The change in $T_{gc}$ is a measured value, which is not desired to estimate in this work. Hence, the change in $T_{gc}$ is considered as an input for the system identification method instead of an output for the system identification method.

There are several system identification methods capable of estimating a linear model online. In this work an online subspace method is utilized as it avoids the risk of getting stuck in a local minimum for non-convex systems and as it is built upon numerically robust and efficient algorithms (Lennart, 1999; Katayama, 2006). The employed subspace method is described in Andreasen et al. (2021).

### *3.2 Training criteria*

One of the challenges of utilizing a data-driven model is to guarantee that an accurate model of the unknown underlying system is identified. Here, we discuss the requirements for model estimation of the considered system:

- *Excitation:* The measured signals from industrial refrigeration systems exhibit an inherent excitation as the system continuously is exposed to varying external as well as internal disturbances (see fig 2). One can, additionally, add a pseudo random binary sequence (PRBS) signal to the gas cooler's fan speed to ensure excitation.
- *Stability*: The gas cooler dynamic is stable. Hence, the identified model's eigenvalues are required to be within the unit circle.
- *Accuracy*: The difference ($\epsilon$) between the estimated output ($\tilde{y}$) with the measured output ($y$) shall be very small, i.e. for a small $\epsilon$ following should be valid:

$$\epsilon > |\tilde{y} - y| \tag{3}$$

- *Causality*: In a real application, actuators might saturate for a short period of time. A saturated value does not contain excitation and therefore it can result in poorly performing models. Hence, the data utilized for training the model should not include saturated actuator values. In practice, the training can be stopped until the actuator is no longer saturated or the model could be cleared depending on how long the actuator has been saturated.
- *Sample Time and sample numbers*: the "best practice" in system identification recommends that the sample time $T_s$ should be $T_c \leq 0.1\tau$ where $\tau$ is the process time constant. Deep knowledge of the general dynamics of these systems enable us to use a qualified initial guess for the system time constant $\tau_{guess}$. We choose the number of samples to be 100. The sample time will be then chosen accordingly.

## 4. ACTIVE FAULT TOLERANT CONTROL OF AMBIENT TEMPERATURE SENSOR

The proposed AFTC scheme is illustrated in fig. 4. Four different tasks, represented by their respective blocks in the figure, are performed within this scheme. the $D/N$ signal is a binary signal indicating Day/Night operation and can be generated by either internal clock of the controller or by analyzing the ambient temperature $T_{amb}$. During night operation the "Online subspace identification" block is active and provides an estimate of the parameters for the model that is used in the "Predictor" block. During day operations the "Predictor", "Fault Detection", and "Correction" blocks are active. The functionality of these blocks will be described in more details in the following subsections. The estimated model, in the "Predictor" block, is a linear model but the underlying system is nonlinear. Hence, a new model is identified by the online identification algorithm every night such that the seasonal change and degradation (or replacement) of components are accounted for. Note, that the current model is only replaced with the newly identified model if it has a better fit than the current model.

### 4.1 The Predictor block

Based on the derived dynamics in eq. (2), section 3, the following first order discrete-time model of the underlying system is considered:

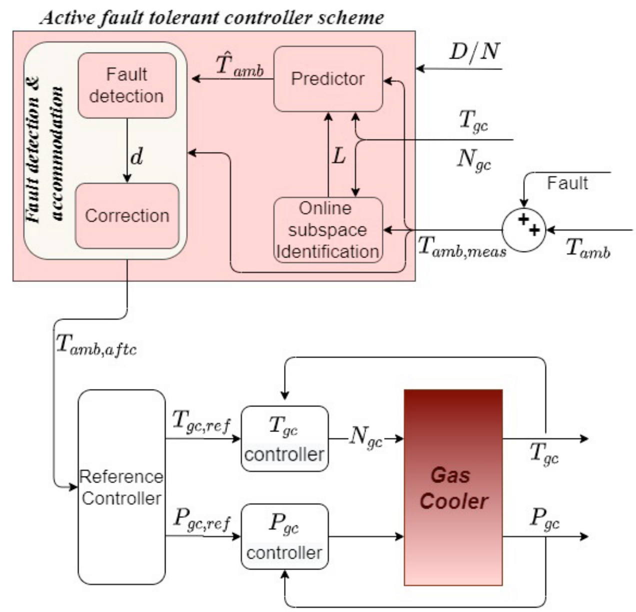


Fig. 4. The active fault tolerant controller scheme.

$$\hat{T}_{amb}(k) = L_{yp}\hat{T}_{amb}(k-1) + L_{up}\begin{bmatrix} N_{gc}(k-1) \\ T_{gc}(k-1) \end{bmatrix} + L_{uf}\begin{bmatrix} N_{gc}(k) \\ T_{gc}(k) \end{bmatrix} \tag{4}$$

where the measured variables are the fan speed ($N_{gc}$), which describes the air mass flow, $T_{gc}$, and $T_{amb,meas}$. It is noted that during the night operations ambient temperature operates without fault, i.e. $T_{amb,meas} = T_{amb}$. The parameters to be estimated are:

$$L = [L_{up} \; L_{yp} \; L_{uf}]$$

with $L_{up} \in R^{1\times2}$, $L_{yp} \in R^{1\times1}$ and $L_{uf} \in R^{1\times2}$.

### 4.2 Fault detection block

There are several methods for fault detection and diagnosis, see e.g. Ding (2014); Blanke et al. (2016). In this paper a simple threshold for evaluating the residual ($\xi(k) = T_{amb,meas}(k) - \hat{T}_{amb}(k)$) is applied. A threshold ($\theta$) for detecting the ambient temperature measurements is set based on the value of $\epsilon$ in eq. (3) . The decision function ($d$) is then defined as:

$$d(k) = \begin{cases} 1 & \text{if } \theta < \xi \\ 0 & \text{if } \theta \geq \xi \end{cases}$$

*Remark:* More advanced statistical based methods have been considered but the chosen method was evaluated to be sufficient due to the large signal to noise ratio.

### 4.3 Correction block

The main idea with the correction block is to ensure a bump-less transfer from the actual measurement of the ambient temperature to it's estimated value (and vice versa) based on the outcome of the "Fault detection" block. The input signal to the "Reference Control" block is calculated as:

$$T_{amb,aftc}(k) = (1 - \zeta(k)) \cdot T_{amb,meas}(k) + \zeta(k) \cdot \hat{T}_{amb}(k)$$

where $\zeta(k)$ is the output of a low pass filter:

$$\zeta(z) = W(z) \cdot d(z)$$

### *4.4 Stability*

Upon detecting fault the AFTC scheme introduces an outer loop on the gas cooler system. The outer loop consists of the first order model in the "Predictor" block and the low pass filter, $W(z)$, in the "Correction" block.
Providing analytical stability for the resulting system is impractical as the dynamic of a given gas cooler is dependent on a number of factors, such as dimensions, used material, design, type of refrigerant, etc. and is inherently nonlinear. It should be noted that the gas cooler dynamics is stable albeit being nonlinear.
Therefore, we carry out the following tasks to avoid instability situations:
- *Predictor model*: The resulting model is required to be stable (see sec 3.2). Furthermore, the model parameters will be updated every night and the resulting model will only be accepted if it provides a better prediction than the previous model.
- *Switching frequency*: Fast switching between the real measurements and the estimated temperature may potentially cause instability. To avoid this scenario the time constant ($\tau_W$) of the low pass filter $W(z)$ is chosen according to the following procedure: In the gas cooler two main close loops describe the dynamics:

$$H_1(s) = \frac{T_{gc}}{T_{gc,ref}}, \quad H_2(s) = \frac{P_{gc}}{P_{gc,ref}},$$

Lets denote the dominating time constants in these systems by $\tau_{T_{gc}}$ and $\tau_{P_{gc}}$. The dynamics related to the air side is always slower than the pressure side, i.e. $\tau_{T_{gc}} > \tau_{P_{gc}}$. Fast switching, and hence instability, is avoided by choosing

$$\tau_W > 3.\tau_{T_{gc}}$$

## 5. RESULTS

Experimental data from a fully functional supermarket, belonging to a customer in Portugal, is used to validate the functionality of the different blocks in the AFTC scheme. However, due to practical as well as the legal reasons it was not possible to close the loop, i.e. use the corrected signal instead of the original measurements when fault was identified. Thus, to validate the closed loop performance of the AFTC scheme a simulation is utilized instead.

### *5.1 Experimental data*

Eight one-week data-sets are available from the system described in section 2. The first approximately 60 hours of the first week, where a model trained is shown in Fig. 5 where the temperature of the refrigerant at the outlet of the gas cooler ($T_{gc}$) is shown in blue. The measured ambient temperature ($T_{amb,meas}$) is shown in red and the corrected ambient temperature ($T_{amb,aftc}$) proposed by the AFTC scheme is shown in yellow. Note, that the AFTC scheme is not active before an model has been identified. A model is derived at approximately 30h. The two vertical purple lines indicate the interval where a model was trained. Sampling time of the data is 60 $s$ and no excitation signal was applied to the system since it is a fully functional supermarket store. The inherent excitation nature of the involved signals were enough for the system identification method to function. The model parameters were estimated after 480 samples and the calculated time constant found to be 459 second.

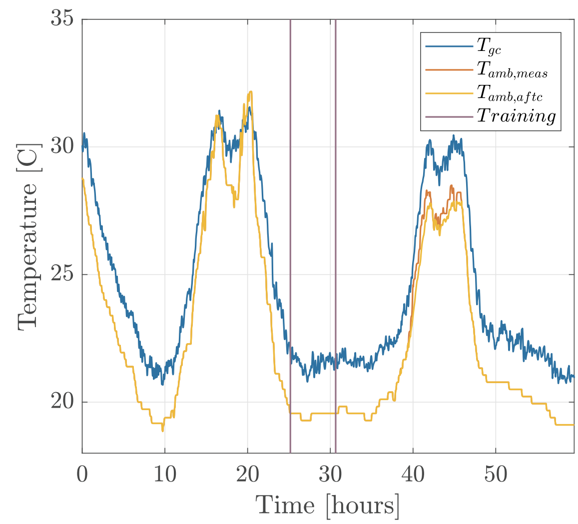


Fig. 5. Illustration of the experimental data and associated results from the AFTC scheme for the first 60 hours, where a model is trained. The two purple lines indicate the interval where the model was trained. Hence, the AFTC scheme is active after approximately 30h. The refrigerant temperature at the outlet of gas cooler ($T_{gc}$) is shown in blue, the measured ambient temperature ($T_{amb,meas}$) is shown in red and the output from the AFTC scheme ($T_{amb,aftc}$) is shown in yellow.

Fig. 6 shows the residual of the measured ambient temperature and the estimated ambient temperature (i.e.

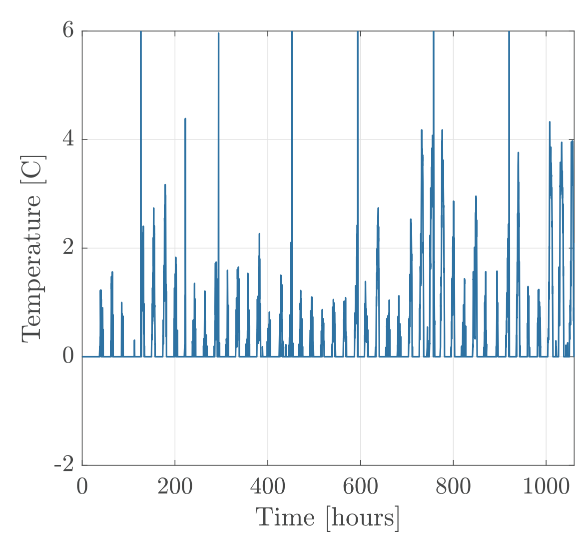


Fig. 6. Illustration of the experimental data and associated results from the AFTC scheme showing the difference between the measured and estimated ambient temperatures (i.e. $T_{amb,meas} - \hat{T}_{amb}$).

$T_{amb,meas} - \hat{T}_{amb}$) for the joint 8 weeks of data. Between each data-set the measurements have a time gap. Hence, a jump in between the data-sets occurs. Most days the AFTC proposes a small correction (less than two degree Celsius) to the measured ambient temperature ($T_{amb,meas}$). However, in some of the days, where the weather has been warm, the corrections proposed by the AFTC are quite significant.

### 5.2 Simulation validation

The algorithm's closed loop performance is validated on a simulation model of a $CO_2$ booster refrigeration system (see (Andreasen et al., 2019)). The exact same settings for the AFTC scheme are utilized. The upper plot in Fig. 7 shows the true ambient temperature ($T_{amb}$, in blue), the measured ambient temperature ($T_{amb,meas}$, in red) and the corrected ambient temperature measurement ($T_{amb,aftc}$, in yellow). Note that $T_{amb,meas}$ and $T_{amb,aftc}$ are on top of one another unless a correction is performed by the AFTC scheme. The lower plot shows the day and night detection (in red) and the training signal (in blue). The major difference from running the AFTC scheme in the simulation rather than on experimental data is that the corrected temperature ($T_{amb,aftc}$) is applied to the system instead of the measured ambient temperature. In the simulation a fault emulating direct and/or indirect heating from the sun on the ambient temperature sensor is present the first three days. The remaining days no fault is applied. The model parameters were correctly estimated during the training period, indicated by the vertical blue lines. 192 samples were utilized for training the model corresponding to 48 minutes of training. The results, illustrated in Fig. 7 show that the AFTC scheme efficiently corrects the ambient temperature measurement fault on the third day.

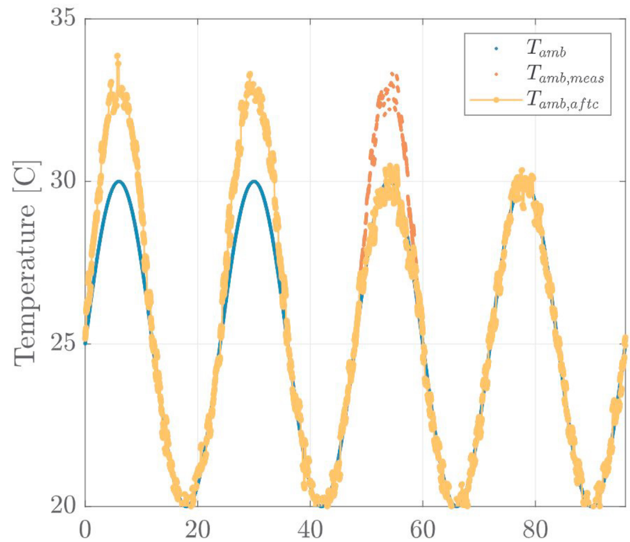


Fig. 7. Illustration of the simulation result of the AFTC. The plot shows the true ambient temperature ($T_{amb}$, in blue), the measured ambient temperature ($T_{amb,meas}$, in red) and the corrected ambient temperature ($T_{amb,aftc}$, in yellow). The training period is between 37h to 38h.

## 6. CONCLUSIONS

In this paper an active fault tolerant controller scheme for detecting and correcting the faulty measurements from an ambient temperature sensor, which is exposed to direct and/or indirect heating from the sun, is proposed. The AFTC is designed in a plug and play manner, where the underlying unknown system dynamics are identified through an online (subspace) identification algorithm. To ensure the validity of the estimated model parameters a set of criteria were proposed. The identified model is utilized to predict the ambient temperature, which is then used to determine whether the measurements are faulty. Depending on the detection results the correction block provides the correct signal to the reference control block in a bump-less manner. The AFTC scheme is validated in an open loop setting on experimental data, where it exhibits a promising ability to estimate and propose realistic corrections of the faulty ambient temperature measurement. The closed loop properties are validated though simulation where the AFTC scheme corrects faulty ambient temperature measurements. Thus, enhancing control reliability and ensures optimal operation of the supermarket refrigeration system.

## REFERENCES

Andreasen, G., Izadi-Zamanabadi, R., and Stoustrup, J. (2021). Virtual refrigerant charge sensor for booster refrigeration systems. *International Journal of Refrigeration*, 122, 59–68.

Andreasen, G., Stoustrup, J., Izadi-Zamanabadi, R., Pardiñas, Á.Á., and Hafner, A. (2019). Data-driven modeling of a $co_2$ refrigeration system. In *2019 American Control Conference (ACC)*, 5385–5390. IEEE.

Behfar, A., Yuill, D., and Yu, Y. (2017). Automated fault detection and diagnosis methods for supermarket equipment (rp-1615). *Science and Technology for the Built Environment*, 23(8), 1253–1266.

Behfar, A., Yuill, D., and Yu, Y. (2018). Supermarket system characteristics and operating faults. *Sci. and Tech. for the Built Environment*, 24(10), 1104–1113.

Blanke, M., Kinnaert, M., Lunze, J., and Staroswiecki, M. (2016). *Diagnosis and Fault-Tolerant Control - Third Edition*. Springer.

Ding, S.X. (2014). *Data-driven design of fault diagnosis and fault-tolerant control systems*. Springer.

Ge, Y. and Tassou, S. (2011). Performance evaluation and optimal design of supermarket refrigeration systems with supermarket model "supersim". part ii: Model applications. *Int. jour. of refrigeration*, 34(2), 540–549.

Katayama, T. (2006). *Subspace methods for system identification*. Springer Science & Business Media.

Kauf, F. (1999). Determination of the optimum high pressure for transcritical co2-refrigeration cycles. *International Journal of Thermal Sciences*, 38(4), 325–330.

Kim, S.C., Won, J.P., and Kim, M.S. (2009). Effects of operating parameters on the performance of a co2 air conditioning system for vehicles. *Applied Thermal Engineering*, 29(11-12), 2408–2416.

Lennart, L. (1999). System identification: theory for the user. *PTR Prentice Hall, Upper Saddle River, NJ*, 1–14.

Yang, L., Li, H., Cai, S.W., Shao, L.L., and Zhang, C.L. (2015). Minimizing cop loss from optimal high pressure correlation for transcritical co2 cycle. *Applied Thermal Engineering*, 89, 656–662.